30th Annual International IEEE EMBS Conference
Vancouver, British Columbia, Canada, August 20-24, 2008

# Cross Correlation and Scatter Plots of the Heart Rate Variability and R-Peak Envelope as Features in the Detection of Obstructive Sleep Apnea

Mohammad Al-Abed[1], Khosrow Behbehani[1], John R. Burk[2], Edgar A. Lucas[2], and Michael Manry[3]
[1] Bioengineering Department, University of Texas at Arlington and University of Texas Southwestern Medical Center at Dallas. [2] Sleep Consultants, Inc. Fort Worth Texas. [3] Electrical Engineering Department, University of Texas at Arlington.

*Abstract*— **Interbeat heart rate as measured by the RR interval (RR) and R-Peak Envelope (RPE) are two signals that can be extracted from an Electrocardiogram (ECG) with relative ease and high reliability. RR and RPE have been shown to carry markers for detecting sleep disordered breathing (SDB). In this pilot study, we explore the cross correlation of RR and RPE in normal and SDB patients. Nocturnal ECG from 7 normal subjects and 7 SDB patients were used to obtain RR and RPE. The results revealed that the cross correlation of RR and RPE signals is significantly different between normal subjects and SDB patients ($p < 2\times10^{-6}$). Furthermore, a new scatter plot of RR vs. RPE was developed. Optimum features from the RR vs. RPE scatter plot were extracted and used as input to a multilayer perceptron (MLP) classifier to distinguish between normal and SDB subjects, The detection sensitivity, specificity and accuracy for the training data set were 95.0%, 100.0%, and 97.5%, respectively; and for the test data were 76.6%, 93.2%, and 84.7%, respectively.**

*Keywords*— **ECG, Sleep Disordered Breathing, Heart Rate Variability, R-Peak Envelope, Cross Correlation, Multi-Layer Perceptron**

## I. Introduction

It is estimated that sleep-disordered breathing (SDB) has a prevalence of 5% in middle-aged U.S. population [1]. It is thought that SDB is associated with memory dysfunction and cardiac disease. It also negatively affects productivity and quality of life. Further, it is estimated that SDB is widely under diagnosed in the population; this is in part due to the cost and limited availability of nocturnal polysomnography (PSG) which is the accepted method of diagnosing SDB. Cost effective and more accessible means to screen the population for SDB are highly desirable. Obstructive Sleep Apnea (OSA) is one of the most prevalent SDB in the population.

Previous studies [2-4] have shown the possibility of screening for SDB using overnight ECG recordings. Different algorithms have been developed to extract reliable markers from ECG signals including heart rate variability (HRV), R-wave attenuation (RWA), and power spectral analysis of particular frequency bands. The use of HRV is appealing, as it reflects the autonomic response to apnea episodes. One study has pointed to combining different temporal statistical features from HRV and RWA to improve the detection rate [3]. Different groups tried to qualitatively describe time-frequency plots of HRV during an international challenge for the detection of SDB using ECG signals [2].

Considering that HRV and RWA both change when OSA is present, we examined the cross correlation of the time series of the temporal distance between consecutive R-peaks (RR) and the time series forming the envelope of the amplitude of the R-peaks (RPE) as a possible marker for distinguishing normal versus sleep disordered breathing.

## II. Methodology

Nocturnal polysomnography (NPSG) recordings were collected at an accredited sleep lab (Sleep Consultants Inc., Fort Worth, TX) and scored using Rechtschaffen and Kales method by a certified sleep specialist who was blind to the objective of this study. Table I summarizes the subject population demographics.

TABLE I
SUBJECT DEMOGRAPHICS OF THE NORMAL AND OSA GROUPS INCLUDING THE APNEA/HYPOPNEA INDEX

| Subject group (N) | Number of males/females | Age (mean ± std) | BMI (mean ± std) | AHI (mean ± std) |
|---|---|---|---|---|
| NOR (7) | 5/2 | 43.00 ± 8.60 | 24.70 ± 4.32 | 4.43 ± 3.60 |
| OSA (7) | 2/5 | 51.14 ± 9.75 | 34.24 ± 6.99 | 38.71 ± 18.85 |

As part of the nocturnal PSG recording, ECG Lead I was digitally recorded at 1 kHz sample rate. It was used to extract both the RR and RPE time series [3]. The data was parsed into epoch of 900-seconds (15 min) length, to capture very low RR variations (~0.001Hz) as recommended in previous investigations [5]. Fifty six epochs were used from 7 normal subjects and 7 OSA patients (4 epochs per each subject). The RR and RPE were interpolated using cubic spline technique, and the resulting function was uniformly sampled at 1 Hz.

*Normalization*: From the RPE time series, the maximum and minimum values ($RPE_{\max}$, $RPE_{\min}$) are obtained for the whole population of all 56 epochs. The time series are then normalized to fall into a range of [0, 1] using the following normalization Eq. (1):

$$RPE_{N_{m,i}} = \frac{RPE_{m,i} - RPE_{\min}}{Range(RPE)} \quad \text{..... Eq. (1)}$$

where $Range(RPE) = RPE_{\max} - RPE_{\min}$, $RPE_{m,i}$ is the $i$-th RPE value ($i$ = 1, 2, …, 899) from the $m$-th epoch

($m$ = 1, 2, …, 56), and $RPE_{N_{m,i}}$ is the $i$-th normalized RPE value from the $m$-th epoch. It is noted that since each two consecutive R-peaks produces one RR interval, a 900 second epoch sampled at 1 Hz produces 899 points. Hence, 899 instead of 900 values of RPE are used.

The same normalization computation is applied to the RR values to obtain the RR time series, using the following Eq. (2):

$$RR_{N_{m,i}} = \frac{RR_{m,i} - RR_{\min}}{Range(RR)} \quad \text{..... Eq. (2)}$$

where $Range\,(RR) = RR_{\max} - RR_{\min}$, $RR_{m,i}$ is the $i$-th RR value from the $m$-th epoch, and $RR_{N_{m,i}}$ is the $i$-th normalized RR value from the $m$-th epoch.

To study the combined effect of changes in RR and RPE several features were considered.

*Cross Correlation between RR and RPE*: The cross correlation between RR and RPE ($R_{xy}(m)$) using Eq. (3) for all normal and OSA epochs was computed as:

$$Rxy(m) = \sum_{n=0}^{898} RR(n-m) \cdot RPE(n) \quad \text{..... Eq. (3)}$$

where $m$ is the delay and ranges between -898 to 898. Figure-1 shows the mean and standard error of means (SEM) of ($R_{xy}(m)$) for the 28 normal epochs and the mean and SEM of ($R_{xy}(m)$) for the 28 OSA patient epochs.

*Scatter Plots of RR vs. RPE*: Scatter plots of RR vs. RPE series were studied. These plots reveal the difference in the distribution, intensity and location of (RR, RPE) pairs for each heart beat. Figure-2 shows an example of scatter plot of RR vs. RPE from a 15-min epoch taken from a normal subject (AHI =6 events per hour). Figure-3 shows an example of scatter plot of RR vs. RPE from a 15-min epoch taken from an OSA subject (AHI = 70 events per hour).

In examining the RR vs. RPE scatter plots discriminatory features that potentially aid in the detection of OSA were investigated. We found that the calculation of the position of two centroids of the scattered data provided the highest decimator power. The locations of the centroids for each epoch are calculated by minimizing the following function:

$$E = \sum_{n=1}^{2} \sum_{i=1}^{899} (P_i - C_n)^2 \quad \text{..... Eq. (4)}$$

where $P_i$ is the ($RR_i$, $RPE_i$) pair, $C_n$ is the location of the centroid $n$ at ($x_n$, $y_n$), and through an iterative heuristic algorithm is changed until the error function $E$ converges [6].

From each centroid, four features can be extracted: its x and y coordinates, and its polar coordinates $\rho$ and $\theta$, where $\rho = \sqrt{(x^2 + y^2)}$ and $\theta = \tan^{-1}(y/x)$. Figure-4 shows the location of the centroids and their corresponding

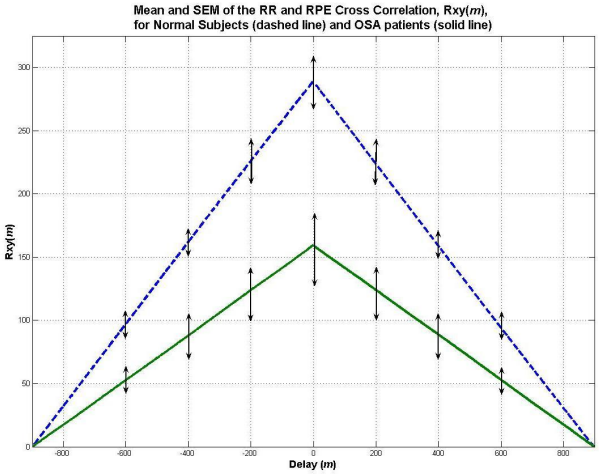


Figure 1: Mean and SEM of the cross-correlation function, $R_{xy}(m)$, of RR and RPE signals for normal subjects (dashed line) and OSA patients (solid line).

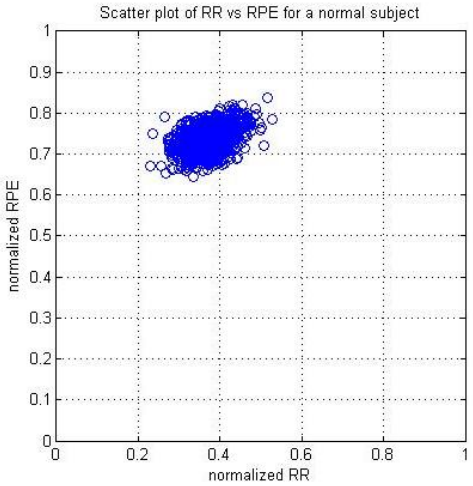


Figure 2: A scatter plot of normalized RR vs. RPE signals for 899 points representing 15 min of overnight ECG LI recordings for a normal subject, with an overall AHI of 6 events per hour.

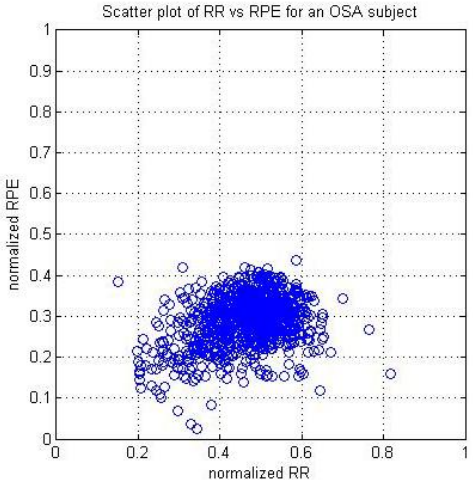


Figure 3: A scatter plot of normalized RR vs. RPE signals for 899 points representing 15 min of overnight ECG LI recordings for an OSA patient, with an overall AHI of 70 events per hour

extracted features from a scatter plot of RR vs. RPE for the epoch illustrated in Figure-3 above.

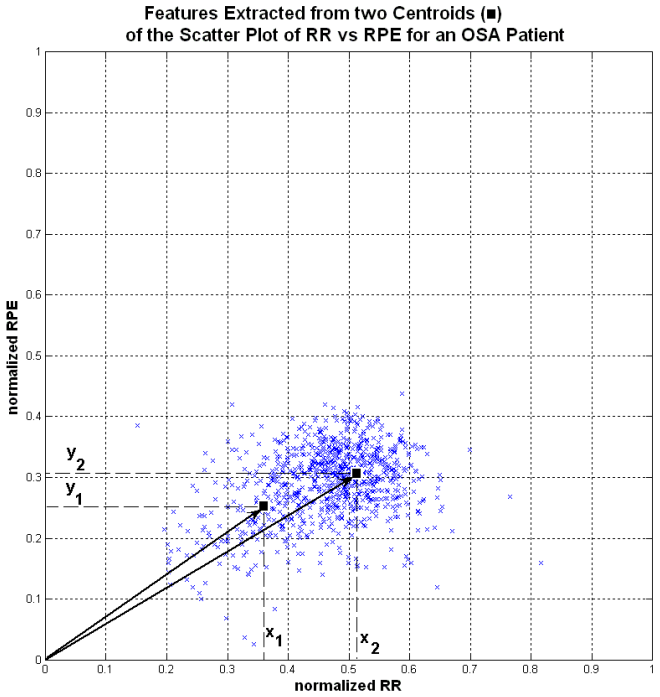


Figure 4: A scatter plot showing the location of the two centroids used to characterize the epoch for further classification. Epoch is the same as the one in Figure 3.

Each epoch now is characterized by 8 features extracted from the location of the two centroids. For a given clips $m$, these features are $x_{1,m}$, $y_{1,m}$, $\rho_{1,m}$, $\theta_{1,m}$, $x_{2,m}$, $y_{2,m}$, $\rho_{2,m}$, $\theta_{2,m}$. We add to these features the cross correlation value at zero delay, $Rxy_m(0)$, for each epoch's features. These constitute 9 features per epoch that can be used as an input vector to an optimized classifier, such as a Multilayer Perceptron (MLP), which has shown agreeable discriminatory results in our previous work [7].

*Multilayer Perceptron Classifier*: A MLP is a form of a feed-forward (FF) neural network. A FF NN is one that does not have any of its frontward layer outputs feeding back into a previous layer's input. Its simple structure allows for relatively easy training, using conventional back-propagation (BP) tainting algorithms. It has been shown that MLP classifiers are very effective in image classification applications [8, 9].

A three layer MLP was used for in this study which had an input, hidden and an output layer. The input layer had a number of nodes equal to the dimension of the input vector. The output layer consisted of one node, accounting for a possibility of only 2 classes to be classified. The number of units in the hidden layer, $N_h$, was found by training the network. Besides changing the number of hidden units, each layer of a MLP had two parameters that were trained to achieve maximum detection: node transfer function and weight vector. Both input and output nodes contained linear transfer function. The hidden layer consisted of a hyperbolic tangent sigmoid function [9].

*Training*: Training of a MLP was achieved by fitting the network parameters to the desired output using BP. When training the network via training set containing the features, the network accuracy increases with the number of training epochs, $N_{ep}$. This is characteristic of MLPs, where it has been shown that they can approximate any polynomial [9]. However, the problem of over-fitting arises with increased number of training epochs, since the accuracy of a test set tends to have an optimum $N_{ep}$; after which the accuracy starts to decline [8].

To train all the MLPs, the test feature set was used as input vectors to the MLP. The test set was selected by randomly assigning the epochs present in the dataset into two groups; training and testing. The ratio of the training to testing was set equal to 2:1. With total of 56 epochs, this translated to 42 epochs for training, and the remaining 14 for testing.

The optimum number of hidden units and training epochs ($N_h$, $N_{ep}$ pair) were found using the following method: For each possible $N_h$, the network was trained using the training set consisting of $N_{ep}$ epochs. This process was repeated until the optimum number of nodes was obtained. After the training established the number of nodes, the weights, and bias parameters of the network, the network topology and parameters were fixed and test data set was run to determine the efficacy of the network classifier. This process was repeated (using the fixed network topology) another 50 times, using different training and testing sets. This method allowed for studying the average performance of the MLP for a given $N_h$. The one-step-secant back propagation method was used for training the MLP [8].

*Sensitivity, Specificity, and Accuracy:* The performance of the system is described by.

$$\text{Sensitivity} = \frac{OSA_c}{Total\ OSA\ clips\ tested} \times 100\%$$

$$\text{Specificity} = \frac{NOR_c}{Total\ NOR\ clips\ tested} \times 100\%$$

$$\text{Accuracy} = \frac{OSA_c + NOR_c}{Total\ NOR\ \&\ OSA\ clips\ tested} \times 100\%$$

where $OSA_c$ is the number of correctly detected OSA epochs and $NOR_c$ is the number of correctly detected normal epochs [10].

## III. Results

*Cross Correlation*: We found that the cross correlation, $R_{xy}(m)$, between RR and RPE for normal subjects and OSA subjects is positive. The mean $R_{xy}(m)$ for normal subjects is significantly higher than that of OSA patients. The most significant difference is at zero delay, $R_{xy}(0)$, with a p-value

of $1.9\times10^{-6}$. Figure-5 shows the and the distribution of the cross correlation values for the sample population OSA $R_{xy}(0)$ values.

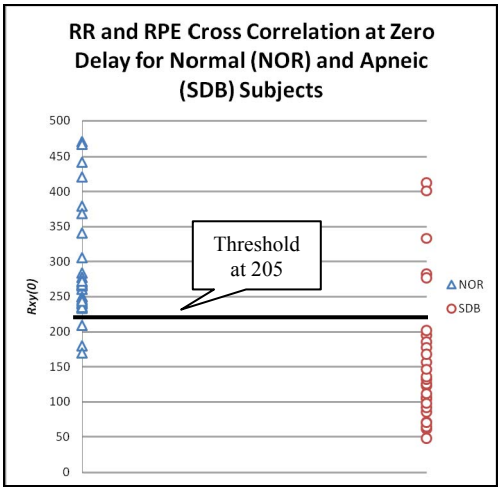


Figure 5: An illustration of the significant difference between normal and OSA patients' cross correlation of RR and RPE at zero lag, $R_{xy}(0)$. A threshold at 205 would achieve an accuracy of 87.5%.

*Feature Selection*: From the proposed nine features (8 centroid features and the $R_{xy}(0)$ values), we found that the features selected using the Piecewise Linear Network were $x_1$, $y_1$, $x_2$, $y_2$, $\rho_1$, $\rho_2$, and $R_{xy}(0)$ and are the optimum features for the classification. These seven features are used as inputs to the MLP classifier.

*Training and Testing Results*: All 28 normal epochs and 28 OSA epochs were randomly divided into training and testing sets: 42 epochs for training and 14 for testing. Using an iterative method to find the optimum number of hidden nodes and optimum number of training epochs, we found that the optimum number of nodes in the hidden layer was $N_h = 10$ and 930 training passes, $N_{ep}$, that would produce the highest accuracy for the testing set. The algorithm employs an early stop technique if the training error drops below $10^{-5}$.

*Detection Results*: Table II shows summary of the training and testing detection results after a 400-run Monte-Carlo simulation.

TABLE II
AVERAGE SENSITIVITY, SPECIFICITY, AND ACCURACY OF MULTILAYER PERCEPTRON CLASSIFIER FOR 400-RUN MONTE-CARLO SIMULATION

| | Training | Testing |
|---|---|---|
| Sensitivity | 95.0% | 76.6% |
| Specificity | 100.0% | 93.2% |
| Accuracy | 97.5% | 84.7% |

## V. DISCUSSION

The cross correlation between RR series and RPE is significantly higher for normal subjects than it is with OSA patients. This signifies a more uniform heart activity in normal patients, where slower heart rate (high RR values) is coupled with a larger R-peak for each QRS complex. However, the lower correlation between RR and RPE for OSA patients can be an indication of lower uniformity in heart function during OSA events.

The proposed centriod features extracted from the scatter plots of RPE and RR when used with MLP as a classifier were shown to be very practical for the proposed OSA event detection scheme, as the training accuracy exceeds 97% and testing accuracies approaches 85%.

## V. CONCLUSIONS

This study has a strong potential of improving the detection accuracy of OSA events by combining RR and RPE signals. The detection algorithm that we present shows that features extracted from combining RR and RPE signals present new possibility for a relatively simple system to screen for OSA in a larger population. Also, further study is needed to examine pathophysiological significance of the low cross-correlation between RR and RPE in OSA patients.

## REFERENCES


[1]. T. Young, M. Palta, J. Dempsey, J. Skatrud, S. Weber, and S. Badr, "The Occurrence of Sleep-Disordered Breathing among Middle Adults", *New England Journal of Medicine*, 328, pp. 1230-1235, 1993.

[2]. T. Penzel, J. McNames, P. de Chazel, B. Raymond, A. Murray, and G. Moody, "Systematic Comparison of Different Algorithms for Apnoea Detection based on Electrocardiogram Recordings", *Medical and Biological Engineering and Computing*, 40, pp. 402-407, 2002.

[3]. P. de Chazel, C. Heneghan, and E. Sheridan, "Apparatus for Detection Sleep Apnea Electrocardiogram Signals", *US Patent Application Publication*, Pub No. US 2003/0055348 A1, March 20, 2003.

[4]. S. Vijendra, K. Behbehani, E.A. Lucas, J.R. Burk, D.N. Burli, and D.H. Dao, "The Use of R-wave morphology in the Detection of Sleep-Disordered Breathing using the Electrocardiogram – A Comparison between Leads," *Conference Proceedings, 26th Annual International Conference of the IEEE EMBS*, 2, pp.3881 - 3884 2004.

[5]. M.F. Hilton, R.A. Bates, K.R. Godfrey, M.J. Chappell, and R.M. Cayton, "Evaluation of Frequency and Time-Frequency Spectral Analysis of Heart Rate Variability as a Diagnostic Marker of Sleep Apnoea Syndrome", *Medical and Biological Engineering and Computing*, 37, pp. 760-769, 1999.

[6]. S. Theodoridis and K. Koutroumbas, *Pattern Recognition*,.Boston: Academic Press, 2003.

[7]. M. Al-Abed, K. Behbehani, M. Manry, J. Burk, and E. Lucas. "A method to detect obstructive sleep apnea using neural network classification of time-frequency plots of the heart rate variability," *Conference Proceedings, 29th Annual International Conference of IEEE-EMBS*, 2007, p6101-6104.

[8]. M. Manry. Jiang Li, Pramod L. Narasimha, and Changhua Yu, "Feature Selection Using a Piecewise Linear Network," *IEEE Transaction om Neural Netwrok*, vol. 17, 2006

[9]. K. Fukunaga, *Introduction to Statistical Pattern Recognition*. Boston: Academic Press, 1990.

[10]. S.R. Suhas, "An Technique for the Detection of Cheyne Stokes Breathing and Obstructive Sleep Apnea using Electrocardiogram", Master's Thesis, Dept of Biomedical Engineering, University of Texas at Arlington, Arlington, TX, USA, 2005.